

Characterization of Mycelium Biocomposites under Simulated Weathering Conditions

Nicholas Schultz, Ajimahl Fazli, Sharmaine Piro, Yuritz Barranco-Origel, Patricia DeLa Cruz, and Dr Yanika Schneider*



Cite This: *ACS Appl. Bio Mater.* 2024, 7, 8408–8422



Read Online

ACCESS |



Metrics & More



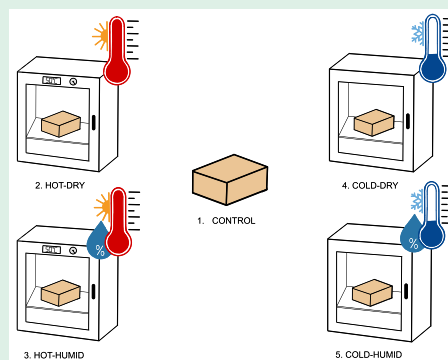
Article Recommendations



Supporting Information

ABSTRACT: Expanded polystyrene (EPS) remains a popular packaging material despite environmental concerns such as pollution, difficulty to recycle, and toxicity to wildlife. The goal of this study is to evaluate the potential of an ecofriendly alternative to traditional EPS composed of a mycelium biocomposite grown from agricultural waste. In this material, the mycelium spores are incorporated into cellulosic waste, resulting in a structurally sound biocomposite completely enveloped by mycelium fibers. One of the main criteria for shipping applications is the ability of a material to withstand extreme weather conditions. Accordingly, this study focused on evaluating a commercially available mycelium material before and after exposure to various weathering conditions, including high and low temperatures at different humidity levels. Fourier transform infrared spectroscopy (FTIR) was performed to examine any transformations in the mycelium structure and composition, whereas scanning electron microscopy (SEM) was used to reveal any changes in the morphology. Similarly, thermogravimetric analysis (TGA) and differential scanning calorimetry (DSC) analyses were conducted to evaluate the thermal behavior, whereas mechanical properties were measured by using shore hardness and Izod Impact testing. Although some irreversible changes were observed due to the exposure to high temperatures, the material exhibited good thermal stability and impact resistance. FTIR analysis demonstrated small changes in the biocomposite structure and protein rearrangement as a result of weathering, whereas SEM revealed some cracking in the cellulose substrate. A combination of low temperatures and humidity resulted in significant moisture absorption, as indicated by TGA and DSC. This in turn decreased the hardness of the fibers by nearly 2-fold; however, the impact strength of the entire biocomposite remained unchanged. Overall, these results provide important insight into the structure–property relationships of mycelium-based materials.

KEYWORDS: *mycelium, agricultural waste, sustainable biomaterials, biocomposites, mycelium-composite, sustainable packaging*



INTRODUCTION

The need for sustainable materials remains pressing as our society struggles to find solutions for waste management. Packaging waste accounts for approximately 30% of the total waste in the United States.¹ Despite the proliferation of single-use plastics in packaging and other applications, no significant changes have been made to recycling processes. Of the 34.5 million tons of plastic waste generated each year, only 9% is recycled.^{2,3} Among these materials, expanded polystyrene (EPS), commonly known as Styrofoam, has been utilized for various packaging and shipping applications, despite being notoriously difficult to recycle.^{4,5} Furthermore, Styrofoam contributes to the spread of microplastics in the ecosystem.⁵ Plastic waste that cannot be recycled is disposed of in landfills, which can then leach into the surrounding environment.^{6–8} Major sources of microplastics entering groundwater include surface runoff, effluent, open dumping, and open burning.⁹ Risks posed by microplastics to marine ecosystems and human health are a consequence of decades of production without alignment on the proper disposal methods.¹⁰ Despite the

versatile nature of polystyrene, novel materials are necessary to address the aforementioned environmental concerns.

In recent years, research efforts have focused on mycelium-based materials due to their unique mechanical properties and biodegradability. Mycelium is the root system of fungi and composed of natural polymers including cellulose, protein, lignin, and chitin.^{11,12} Mycelium typically grows on a substrate made of agricultural waste products or dead organic materials.¹³ The life cycle of the fungi is shown in Figure 1. The cycle begins with the germination of the fungi's reproductive cells, known as spores.^{14,15} Subsequently, hypha or fungal filaments begin to branch out from those spores, creating a dense mycelium network. After some time, the

Received: August 21, 2024

Revised: October 9, 2024

Accepted: November 6, 2024

Published: November 26, 2024



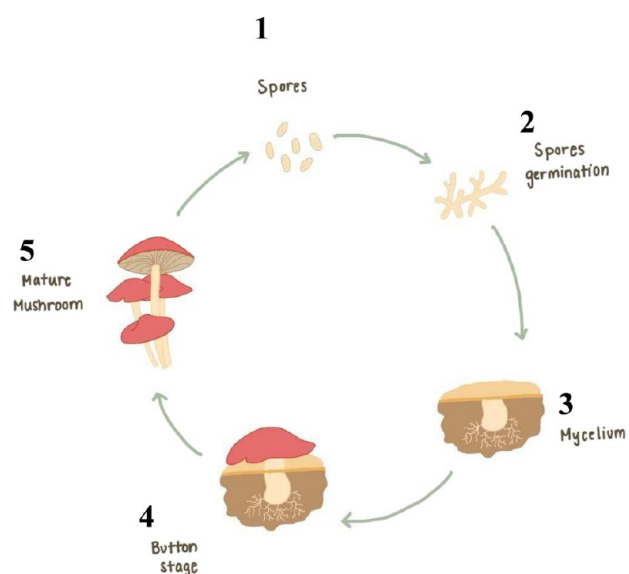


Figure 1. Life cycle of a mature mushroom occurs during five distinct stages.

mycelium roots colonize and ultimately cover the entire surface area of the substrate.¹⁶ Following certain environmental cues, such as changes in temperature and/or humidity, the mycelium matures by focusing its energy into fruiting a mushroom. At the end of the mushroom maturation phase, the gills or underside of the mushroom cap produce spores, completing the cycle and allowing for the cultivation of more fungi.

Mycelium biocomposites generated during the third stage in the life cycle have attracted much attention as a replacement for synthetic plastics.¹⁷ Under ideal temperature and humidity conditions, the mycelium will expand to fit any volume within approximately 5 days, creating a solid structure with the mycelium fibers interwoven throughout the substrate.^{18–20} To halt the maturation and fruition processes, the fully colonized substrate is typically exposed to heat and allowed to dry out.²¹ The resulting material is a biocomposite with a unique combination of a cellulosic substrate that is completely enveloped by a network of mycelium fibers. The physical properties of this biocomposite are similar to those of EPS. In particular, this material is lightweight, porous, and shows reasonable mechanical strength. In addition, the mechanical properties can be modified by varying the nature of the substrate and the mycelia strain.^{22,23} In contrast to EPS, the

mycelium biocomposite is fully biodegradable. Studies have shown it can take only 2 days for the material to begin to break down and 45 days to completely decompose.^{24,25} Given its sustainability and functional properties, mycelium has the potential to replace EPS and mitigate plastic pollution.

Recent advancements in the development of mycelium-based composites for packaging applications have focused predominantly on mechanical properties.^{26–28} Yang et al. examined the relationship between the various strains of mycelia, revealing that the *Ganoderma lucidum* strain exhibited the best performance for making a flexible and strong material.²⁶ Similarly, Joseph et al. created more than 23 fungal strains to understand how biology and processing affect the mechanical response.²⁷ In one of the few studies that examined chemical and thermal properties of mycelium, Jose et al. explored various mycelium manufacturing methods for packaging applications and compared them with EPS.²⁸ Differential scanning calorimetry (DSC) and thermogravimetric analysis (TGA) demonstrated that mycelium biocomposites showed better thermal stability and lower density than did EPS.

To replace EPS, biocomposites must be robust to extreme weather conditions. As mentioned earlier, mycelium biocomposites are known to be affected by environmental conditions, such as temperature and humidity. Much research on mycelium has focused on optimizing the composition of the biocomposite and its degradation, but few studies have examined commercially available mycelium under different weather conditions. Chan et al. evaluated the effect of both humidity and temperature on lab-grown mycelium biocomposites over the course of 35 days.²⁹ After weathering, a decrease in the mechanical strength was observed due to moisture absorption of the wood component. Analysis of its thermal degradation has shown a process of delignification and dehydration when exposed to higher temperatures.^{30,31} Despite efforts in understanding the effect of environmental changes on mechanical properties, to the best of our knowledge, no studies have attempted to correlate mechanical characteristics with chemical, morphological, and thermal changes.

The purpose of this study is to evaluate the effect of various real-world environmental conditions on the properties of commercially available mycelium biocomposite. Extreme conditions such as freezing temperatures, high heat, and high humidity were examined. Unlike previous studies, we focus on both the mechanical properties, as determined by hardness and impact testing, as well as chemical, thermal, and morphological characteristics to provide a more complete picture of the

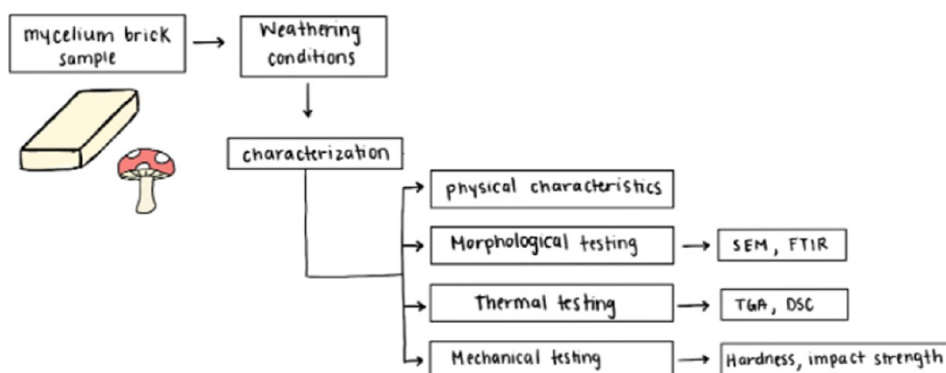












Figure 2. Process flowchart for weathering and characterization of mycelium samples.

Table 1. Physical Characteristics of Mycelium Samples Exposed to Different Conditions

Sample ID	Physical appearance	Texture	Digital Image Cross-section (2x Magnification)	Digital Image Surface (2x Magnification)
Control (1)	Off-white, mycelium layer fully intact and fully coating sample brick	Stiff, styrofoam-like texture, both smooth and rough all around		
Hot-dry (2)	Off-white with yellow hue, irregular and rigid texture, mycelium layer fully intact and fully coating sample brick	Stiff, rubbery texture		
Hot-humid (3)	Tan, very thin mycelium layer all around, inconsistent surface coating	Stiff, styrofoam-like texture, one side smooth, one side rough		
Cold-dry (4)	Off-white, mycelium layer thinner more sheer, the mold imprint is more pronounced compared to controlled	Stiff, bumpy		
Cold-humid (5)	Off-white, mycelium layer thicker foam consistency, mold imprint more faded compared to controlled	Soft, velvety		

transformation in the biocomposite. Past research has shown mycelium to be biodegradable; thus, the capability of this material to withstand extreme conditions is the central focus of this study. These results can help further our understanding of mycelium-based materials with a broad range of applications.

MATERIALS AND METHODS

The experimental method is divided into three main components consisting of sample preparation, weathering, and analytical testing, as shown in Figure 2.

Materials. Mycelium-based packaging was acquired from Paradise Packaging Co. and was stored in the dark at room temperature throughout the experiment. The dimensions of the mycelium samples are 16.25 × 15.9 × 5.1 cm. The samples attained were consistent in shape and had a thickness of 1 mm in the mycelium coating. Eight mycelium bricks from the same lot were purchased and exposed to weathering conditions. According to the supplier, the substrate is composed of hemp hurds.³² The specific mycelium strain is

undisclosed, possibly due to its proprietary nature. Potassium chloride was used as received.

Weathering Simulation. Mycelium samples were exposed to various weathering conditions to simulate real-world shipping environments. As noted by the distributor Mushroom Packaging, mycelium packaging can remain shelf-stable for upward of 30 years under the right conditions.³² Accordingly, ultraviolet light exposure was not included with the weathering parameters as the material is not meant for applications with direct exposure to sunlight.²⁹

A control (1) was tested before weathering on Day 0. The weathering conditions include the following: hot-dry (2), hot-humid (3), cold-dry (4), and cold-humid (5). An incubator (Thermolyne Type 142300) was used to create hot (2) conditions wherein the samples were heated to 50 °C for 7 days. To induce humidity (3), a salt bath was created using 12.3 g of potassium chloride and 200 mL of water in a sealed aluminum vessel. The samples were equilibrated in a sealed aluminum vessel, suspended in the vessel, and then placed in the oven at 50 °C for 7 days.³³ For the cold-dry (4) condition, the samples were placed in an ice-free freezer with a temperature of −19 °C for 7 days. The humid (5) version of the cold conditions was

achieved by wrapping the samples in plastic wrap and then sealing them in aluminum foil to seal residual moisture before placing them in the same freezer for 7 days.³⁴

The four weathering conditions were chosen to emulate extreme, real-world environments. For example, condition (2) simulates arid locations like Saudi Arabia, whereas condition (3) is representative of hot and humid locations such as Thailand. Likewise, extremely low temperatures $-19\text{ }^{\circ}\text{C}$ without humidity (4) are observed in places like Peru, whereas cold-humid conditions are prevalent (5) in Northeast China.

Density. Density (ρ), as determined using eq 1 by measuring the mass (m) of the mycelium sample using a triple beam balance. Volume (V) was determined by measuring the dimensions of the sample using a caliper.³⁵

$$\rho = \frac{m}{V} \quad (1)$$

FTIR Spectroscopy. The surface of each sample was examined in the attenuated total reflection mode by using a Thermo-Nicolet iS50 Fourier transform infrared (FTIR) spectrometer equipped with a Continuum microscope. A diamond crystal was used with a typical depth of penetration on the order of $2\text{ }\mu\text{m}$. The analytical spot size was approximately $100 \times 100\text{ }\mu\text{m}$. OMNIC 9.12 software was used to perform the data analysis.

X-ray Fluorescence Spectroscopy. Elemental compositions were determined using X-ray fluorescence (XRF) using a Rigaku Primus II wavelength dispersive spectrometer (WDXRF), which detects elements with a range from atomic number (Z) 4 (beryllium) through atomic number 92 (uranium) at concentrations from the low parts per million (ppm) range up to 100% by weight. The primary X-ray source comes from a rhodium X-ray tube. The sample analysis is tested using a 20 mm diameter sample holder under a vacuum. Fundamental parameters Standardless quantification software was used for element quantification. ZSX software was used for data processing.

Scanning Electron Microscopy. Scanning electron microscopy (SEM) images are produced by rastering a finely focused electron beam over a sample's surface and using the resulting secondary electrons to modulate the intensity of a display. The samples were examined at 10 kV using SEM with an FEI Quanta 600 SEM equipped with an Oxford EDS system.

Thermogravimetric Analysis. TGA was performed using a TGA TA Instruments TGA5500 for the analysis of thermal degradation of the samples. Measurements were performed using 5–10 mg samples in platinum pans under a nitrogen atmosphere with a temperature range from room temperature to $700\text{ }^{\circ}\text{C}$ and a heating rate of $10\text{ }^{\circ}\text{C}/\text{min}$. The gas was switched to air at $600\text{ }^{\circ}\text{C}$ to burn off any organics.

Differential Scanning Calorimetry. DSC was performed using a TA Instruments Q20 DSC for examining the thermal transitions present in the samples. The specimens were weighed on an electronic balance and then hermetically sealed in aluminum pans. The pan was punctured to release any moisture evaporated during the run. Samples were heated in a temperature range from $20\text{ }^{\circ}\text{C}$ to $250\text{ }^{\circ}\text{C}$ using a ramp rate of $10.00\text{ }^{\circ}\text{C}/\text{min}$. The change in enthalpy was recorded as a function of heat flow/temperature.

Shore Hardness. Shore hardness was evaluated using a PTC Instruments Shore D Scale Durometer for examining the surface hardness using the ASTM D2240–75 standard.³⁶ The test was performed by placing the needle tip of the durometer at various locations of the mycelium surface, followed by the application of slight pressure. The resulting hardness reading was recorded. Three replicate tests were conducted for each sample. The test was performed only on the white component of the sample.

IZOD Impact. The IZOD impact test was performed using a Baldwin Southwark Division Impact Tester. The test determines how much kinetic energy is absorbed by the materials until plastic deformation occurs. The ASTM D4812 standard was consulted in the experimental design.³⁷ A sample with dimensions $2 \times 1 \times 1/2\text{ in.}$ was cut with a ceramic knife, taking care to ensure the sample did not crumble. The IZOD impact test involves the swinging of a pendulum

with a determined weight at the end of its arm, which strikes the specimen that is held securely in a vertical position. The sample was set to face away from the impact, meaning the outer white part was struck. Typically, the sample specimen will have a notch in order to help the sample break when it is struck. In this case, the material was not notch-sensitive, meaning it did not need this component to break. Three replicate tests were conducted for each sample.

RESULTS

Physical Characteristics. Table 1 provides optical images and physical observations of mycelium biocomposites before and after exposure to four weathering conditions. The control sample exhibited an off-white mycelium-rich layer with complete coverage of the substrate. The hot-dry (2) sample had a slight yellow hue and an irregular, rigid texture. Akin to control (1), the mycelium layer was fully intact and completely coated the sample. In contrast, under hot-humid (3) conditions, a dramatic difference in the appearance was observed. The mycelium layer exhibited a darker tan color and was much thinner with an inconsistent surface coating. The mycelium layer of the cold-dry (4) condition appeared to be significantly thinner and more translucent than that of control (1). This is evidenced by the stronger appearance of the mold imprint in these samples compared to that of control (1). In contrast, the mycelium layer of the cold-humid (5) sample had a thicker, foamy consistency, and the mold imprint was less pronounced when compared to the control (1) sample. These results suggest that humidity causes considerable differences in physical appearance.

Chemical Characterization. As shown in Figure 3, the mycelium biocomposite contained two distinct regions: (1)

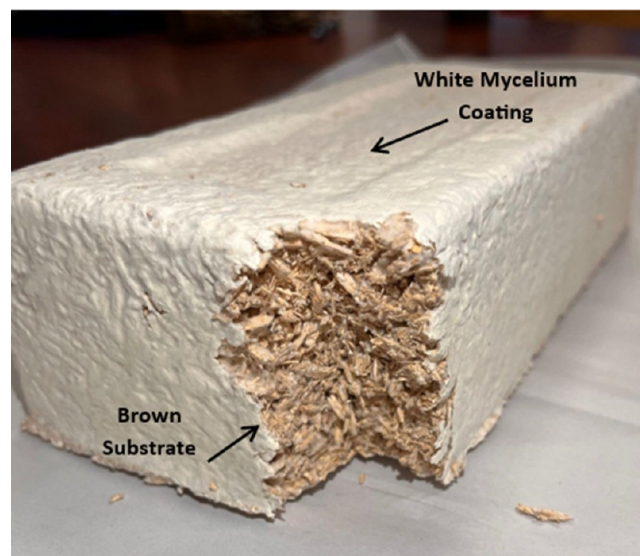


Figure 3. Optical image of mycelium biocomposite revealing the white and brown components.

the mycelium-rich coating identified as the white (W) component and (2) the brownish substrate identified as the brown (B) component. Figure 4 provides a comparison of the FTIR results obtained for the two components, whereas Figures 5 and 6 compare each component with the reference spectra. The white mycelium is primarily composed of a mixture of polyamide or protein (3390 , 1647 , 1544 , 1455 , 1406 , 1317 , and 1250 cm^{-1}) and cellulosic (3290 , 1167 , and 1075 cm^{-1}) components as shown in Figure 5. In contrast, the

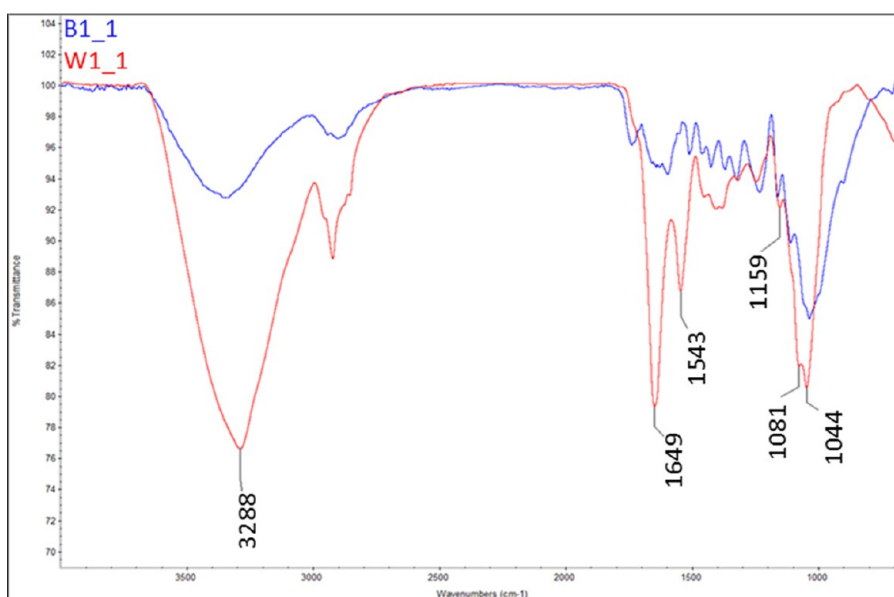


Figure 4. FTIR comparison of white (W1) and brown (B1) components of the control sample. The results suggest that W1 is a mixture of polyamide and cellulose, whereas B1 only contains cellulose.

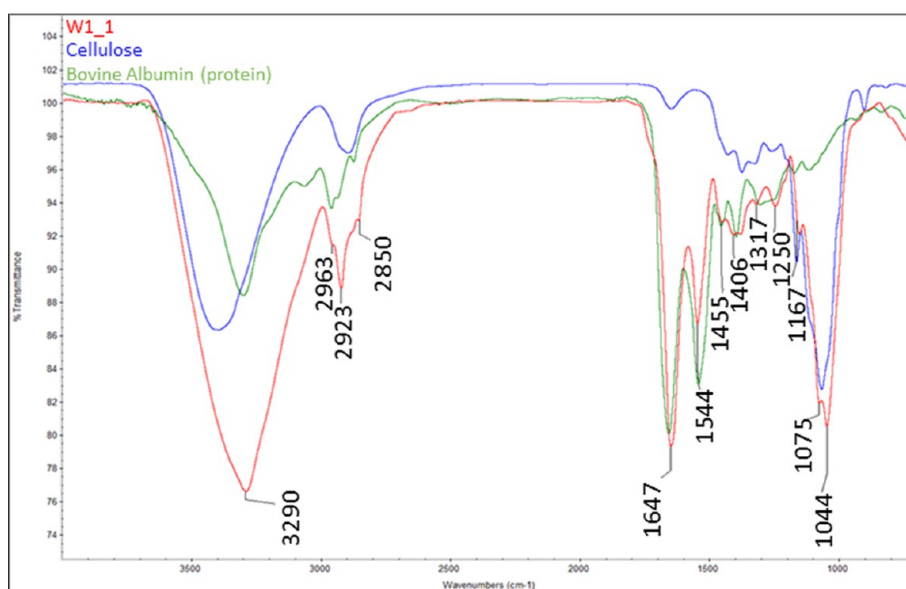


Figure 5. Overlay of the FTIR spectra of the white mycelium component (W1) with reference spectra of a protein (bovine albumin) and cellulose, demonstrating the presence of both polyamide and cellulose species in the white mycelium fibers.

brown component is primarily composed of a cellulosic material similar to wood (Figure 6). These results are consistent with the manufacturer's claim that the substrate is composed of hemp herds, which is a cellulosic material. The peak positions of all vibrations in the white component are provided in Table 2 and found to match literature values.^{38–40}

XRF was used to determine the carbon, nitrogen, and oxygen ratios of two different batches of mycelium biocomposites. As shown in Table 3, some variability is observed in the nitrogen and oxygen contents between the two batches. Nevertheless, the white component showed a higher concentration of nitrogen (5.1–5.3 wt %) compared to that of the brown component (1.9–3.6 wt %), whereas the brown component had a slightly higher oxygen content (51–53 wt %) compared to that of the white component (48–49 wt

%). These results are consistent with FTIR findings of higher concentrations of N-rich protein in the white component.

Next, we examined the effects of all weathering conditions on the composition of the white component, and the results are shown in Figure 7. The main differences among the various spectra are related to changes in the intensity of amide I (1638 cm^{-1}), amide II (1543 cm^{-1}), and cellulose (1043 cm^{-1}) peaks. Note that the amide I band is related to the carbonyl functional group, whereas the amide II band is related to the amino functional group in the polyamide component. Changes in the ratio of amide I to amide II peaks represent changes in the protein structure. Moreover, the amount of cellulose versus polyamide on the surface is represented by the amide I to cellulose ratio.

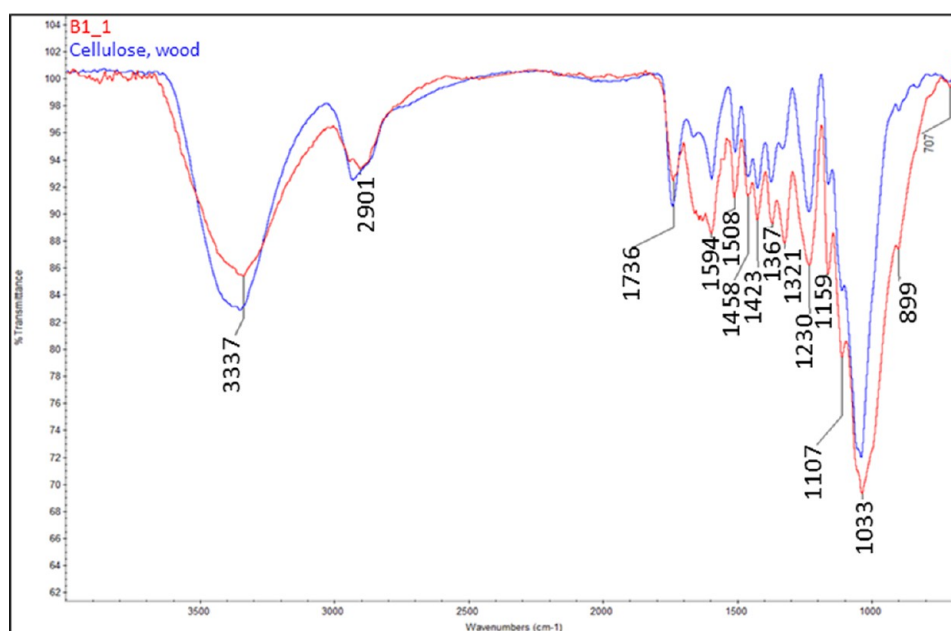


Figure 6. Comparison of the FTIR spectra of brown mycelium component (B1) and a reference spectrum of wood, demonstrating that the B1 can be identified as a cellulosic material similar to wood.

Table 2. FTIR Vibrations Detected in Control White Mycelium (W1) from Figure 5

observed peak (cm ⁻¹)	peak assignment	mycelium component
3290	OH stretching	polysaccharide
2963–2850	CH ₂ stretching	lipid
1647	C=O stretching amide I	protein
1544	C–N stretching Amide II	protein
1455	CH ₂ bending	lipid
1406	C–O–O ⁻ of amino acids and lipids	lipid and protein
1317	In plane bending CO–H	polysaccharide
1250	C–C, C–O and C=O stretching	lignin and polysaccharide
1167	C–O and C–C nonsymmetric stretching	polysaccharide
1075	C–O–C symmetric stretching	polysaccharide
1044	C–O stretching	polysaccharide

Table 3. XRF Results for Both Components of Control Mycelium Biocomposite (1)

component	batch 1 white	batch 1 brown	batch 2 white	batch 2 brown
C	39.7	38.8	42.8	40.8
N	5.30	1.90	5.08	3.62
O	48.9	53.0	47.9	50.7

Four separate measurements were performed on each mycelium sample, and the intensities of the three aforementioned peaks were measured. Figure 8 provides a graphical representation of changes in the mycelium structure due to weathering conditions. For the control (W1) sample, the white component showed an amide I/II ratio of 1.7 ± 0.1 and an amide I/cellulose ratio of 0.9 ± 0.1 . Under hot conditions (W2) and (W3), the amide I/II ratio increased to roughly 1.9 ± 0.1 . This result suggests that the protein component undergoes a rearrangement due to heat, causing the nitrogen-containing functionality to become more prominent on the

surface. Different trends are observed with respect to the amide I/cellulose ratio. While the ratio remained the same under hot-dry (W2) conditions at 0.9 ± 0.1 , the humidity (W3) caused a marked decrease to 0.6 ± 0.1 . This indicates that the combination of humidity and heat results in a change in the amount of cellulose on the surface.

Under cold conditions, the degree of protein rearrangement is lower than that under heated conditions, showing a slightly higher amide I/II ratio of 1.8 ± 0.1 . This indicates that the protein configuration is not as affected by the cold temperatures as it is by hot temperatures. That said, humidity shows a strong effect on the amide I/cellulose ratio of the cold samples, with a decrease to 0.7 ± 0.1 under cold-dry conditions (W4) and a slight increase to 1.0 ± 0.2 under cold-humid (W5) conditions. This suggests that the amount of cellulose on the surface is strongly affected by the humidity level.

MORPHOLOGICAL CHARACTERIZATION

Scanning Electron Microscopy. The morphology of mycelium samples was examined by using SEM before and after exposure to weathering. Figure 9 provides SEM images of control (1) mycelium biocomposites. Mycelium fibers with a diameter of approximately $1 \mu\text{m}$ were detected throughout the cellulose substrate. The fibers are shown in greater detail at a magnification of $4000\times$ in Figure 9c, revealing some variability in the fiber diameter. The effects of various treatments are shown in Figure 10. All conditions except (S) exhibited cracking and other forms of damage to the cellulose substrate, as indicated by orange arrows. In contrast, the cold-humid condition (S) did not show damage to the substrate. Higher magnification images are provided in the Supporting Information in Figures S1 and S2. In addition, the mycelium fiber diameter was measured, and the results of 10 measurements are shown in Figure 11. Fiber diameter slightly increased for all weathering conditions, with W3 showing the greatest increase but also the most variance in the measurements. These results indicate that there were no significant changes in the fiber diameter due to weathering. Altogether, it appears

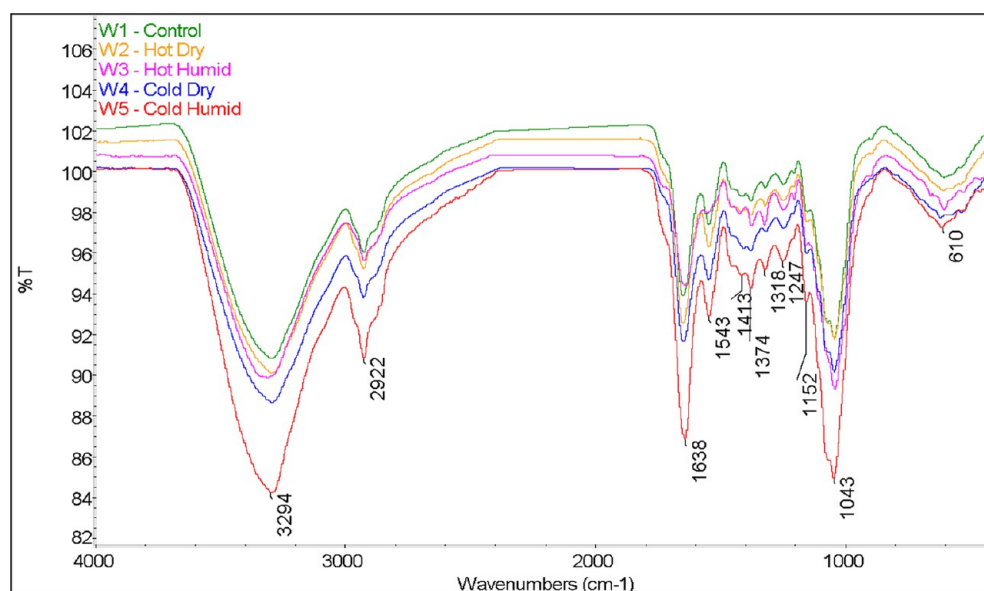


Figure 7. Comparison of FTIR results of the white component: control (W1), hot-dry (W2), hot-humid (W3), cold-dry (W4), and cold-humid (W5).

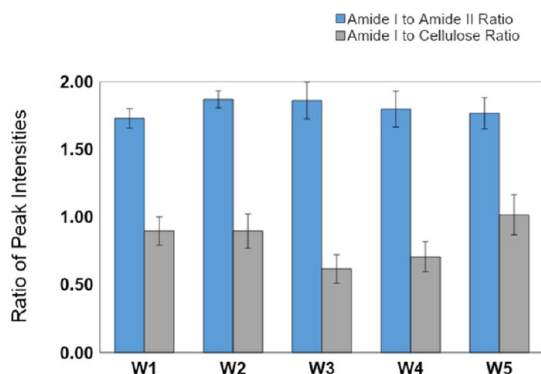


Figure 8. Changes in amide I (1638 cm^{-1}), amide II (1543 cm^{-1}), and cellulose peak (1043 cm^{-1}) ratios of the mycelium biocomposites after various weathering conditions. A minimum of 4 measurements were evaluated for each condition. The results suggest that a combination of extreme weather and humidity exhibits an effect on the amide-to-cellulose ratio, but a less pronounced effect on the amide I-to-amide II ratio.

that the substrate is more affected by the various conditions than the fibers.

■ THERMAL ANALYSIS

Thermogravimetric Analysis. TGA was used to determine the thermal properties of the biocomposite using a method similar to literature procedures.^{18,41,42} Tests were performed on both the white and brown components, and the results are summarized in Figures 12–14. Derivative plots of the biocomposite are included in the Supporting Information in Figures S3 and S4. Biocomposites are expected to absorb a considerable amount of moisture (volatiles), and indeed, 4.3–5.6 wt % moisture was detected in all samples. Likewise, the cellulose substrate may contain inorganic components, which should produce a solid residue after exposure to air above $600\text{ }^{\circ}\text{C}$.⁴³ Our samples averaged approximately 20–30 wt % solid residue, although the sample subjected to hot-humid conditions (B3) contained only 17.8 w % solids. Figures 12 and 13 provide the TGA profiles of the biocomposites, demonstrating one main transition at $\sim 324\text{--}359\text{ }^{\circ}\text{C}$ with another minor transition at $\sim 482\text{--}501\text{ }^{\circ}\text{C}$, which is in line with the two-step decomposition observed in the literature.^{41–46}

The TGA results in Figure 14 represent the relationship between humidity, temperature, and thermal properties of mycelium biocomposites. Exposure to dry conditions (2) and

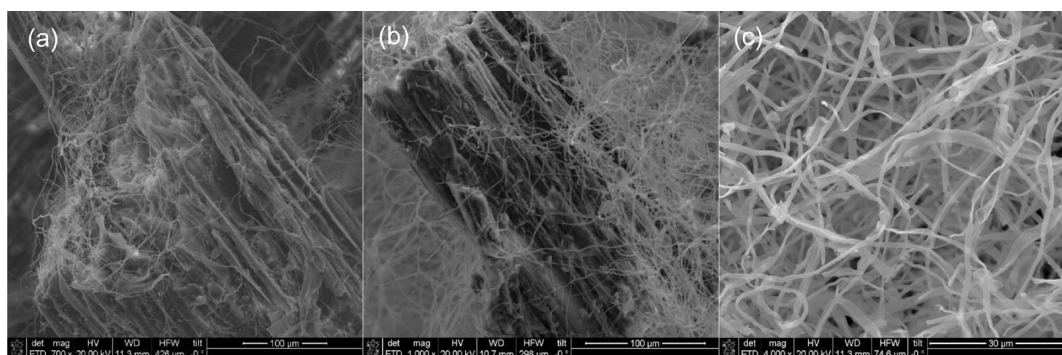


Figure 9. SEM images of control mycelium biocomposite (1) obtained at (a) 700 \times , (b) 1000 \times , and (c) 4000 \times .

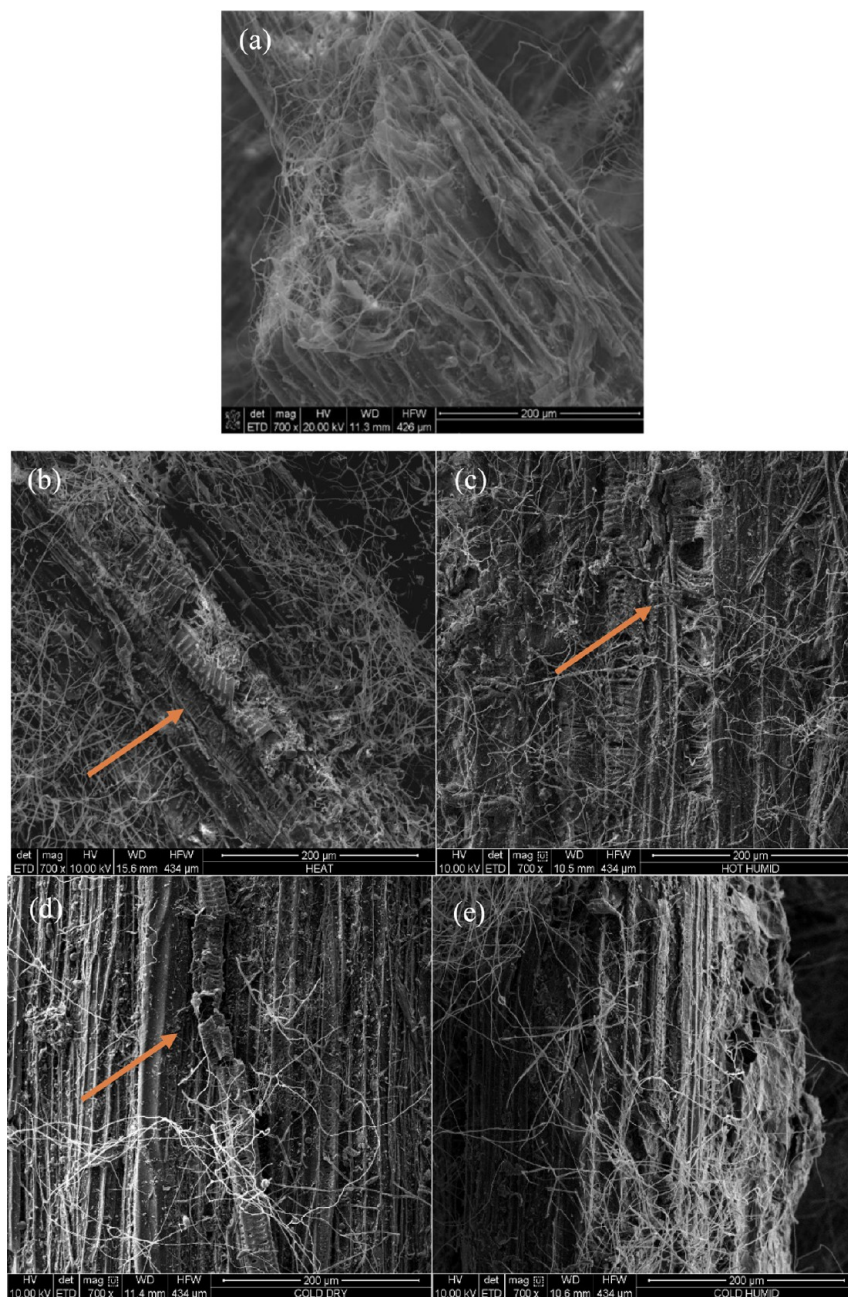


Figure 10. SEM images of the mycelium biocomposite at 700 \times magnification: (a) control (1), (b) hot-dry (2), (c) hot-humid (3), (d) cold-dry (4), and (e) cold-humid (5). Orange arrows represent cracking and other forms of damage to the cellulose substrate.

(4) resulted in a slight decrease in the volatile content of both components. In contrast, when the brown component was exposed to moisture under cold conditions (B5), the volatiles increased from 4.8 to 5.6%. Interestingly, the white fibers did not exhibit significant changes in the volatile species under the same conditions.

Thermal stability of biocomposites was assessed by comparing the $T_{d,5\%}$ (5 wt % mass loss), T_{onset} (onset of degradation), and T_{max} (maximum degradation as determined from the derivative plot). The white component of the weathered samples exhibited higher $T_{d,5\%}$ and T_{onset} under all conditions compared to the control (W1), suggesting higher thermal stability despite the weathering process. Only at peak degradation did the dry conditions (W2) and (W4) show a decrease in the T_{max} suggesting a slight change in the fiber

structure. Unlike the white fibers, the brown substrate showed similar or slightly decreased thermal stability. Namely, the onset of degradation for condition (B2) decreased by nearly 20 $^{\circ}\text{C}$ while remaining unchanged for other conditions. This result suggests that high heat has a deleterious effect on the cellulose substrate. Likewise, T_{max} was reduced by 2.7 $^{\circ}\text{C}$ under hot-humid conditions (B3). No major changes were observed in the cellulose component due to cold exposure. These results indicate that the brown component was more affected by high temperatures but generally remained stable. These results are also consistent with the SEM observation that the substrate was more affected by weathering than the fibers. Note that $T_{d,5\%}$ remained the same for all conditions except conditions (B5) and (W3), wherein significant moisture absorption is convoluted with polymer degradation. The additional moisture

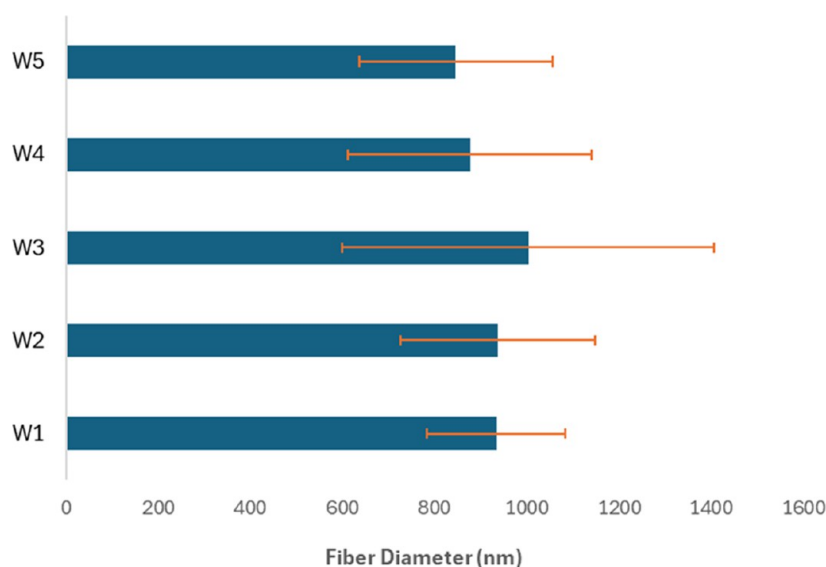


Figure 11. Effect of weathering on mycelium fiber diameter. Fiber diameter slightly increases for hot humid conditions and decreases for cold conditions. The average and standard deviation of 10 measurements are provided. No major changes were observed in the fiber diameter due to weathering.

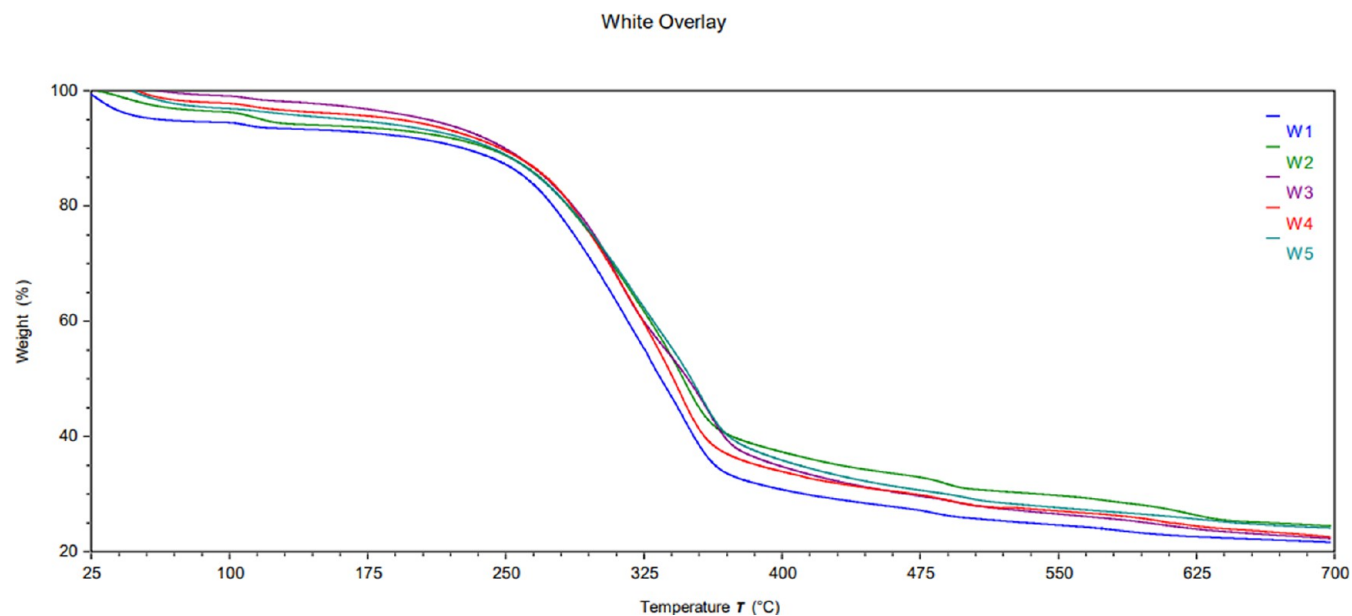


Figure 12. TGA thermogram overlay of the mycelium coating: control (W1), hot-dry (W2), hot-humid (W3), cold-dry (W4), and cold-humid (W5).

gained in the hot-humid condition (W3) must have allowed for better water retention, as it displayed a 78% increase before releasing 5% mass loss.

Interestingly, the residues remained unchanged for all samples except the hot-humid condition (B3), wherein the substrate displayed a sharp 30% decrease. This may indicate that high heat and humidity enhanced the decomposition of the solid organic species that are present in the residues. Heat and humidity can further break down cell structures and lead to quicker decomposition. The exact mechanism of this degradation pathway should be explored in subsequent studies. Overall, changes in the thermal properties of the biocomposite do not appear to significantly deteriorate (in some cases, improving), suggesting that this commercial product is viable for shipping applications.

Differential Scanning Calorimetry. A DSC method was used to evaluate thermal transitions in mycelium biocomposites. The results are provided in Figures 15–17 and Table 4. All samples exhibit two endothermic transitions related to water evaporation at (80–100 °C) and lignin softening (140–160 °C).^{47,48} For the control sample (1), the white component absorbed more moisture than the substrate, as indicated by H_f values of 131.6 and 113.1 J/g for the white and brown components, respectively. Similarly, lignin softening was 10-fold lower for the brown component compared to the white due to a lower amount of lignin in the biocomposite.

DSC results in Figure 17a,b represent the relationship between the temperature and enthalpy of water absorption. Under hot conditions (B2) and (B4), the brown component showed an increase in the temperature of water absorption

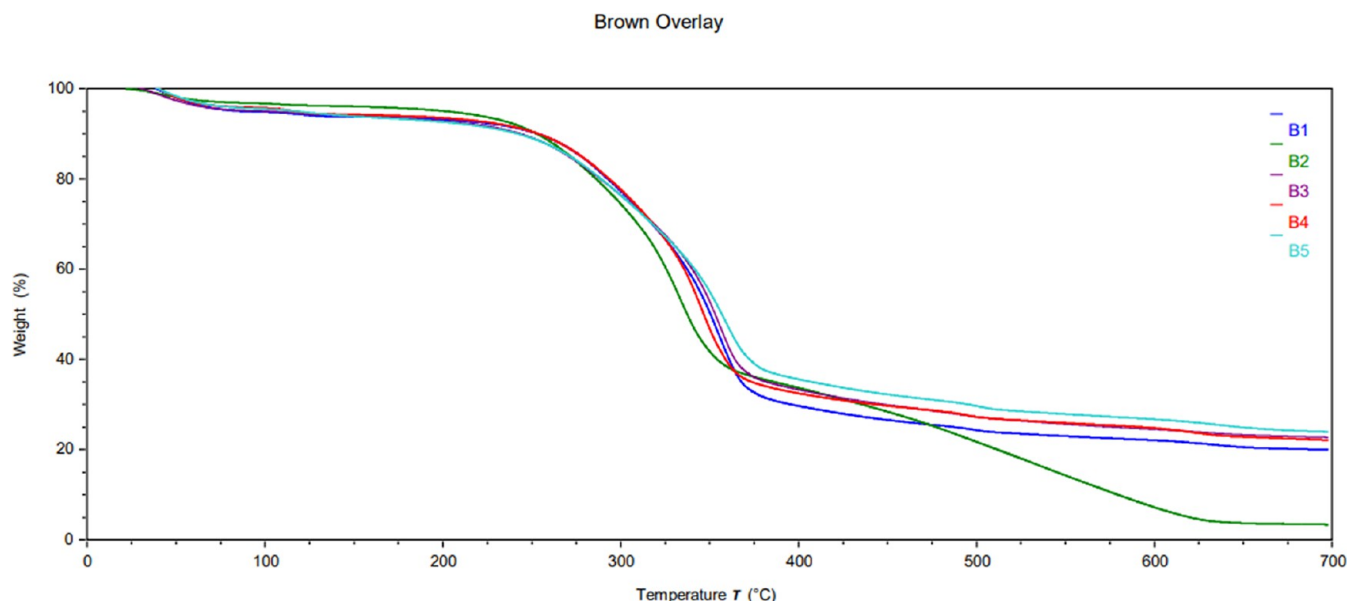


Figure 13. TGA thermogram overlay of the mycelium substrate: control (W1), hot-dry (W2), hot-humid (W3), cold-dry (W4), and cold-humid (W5).

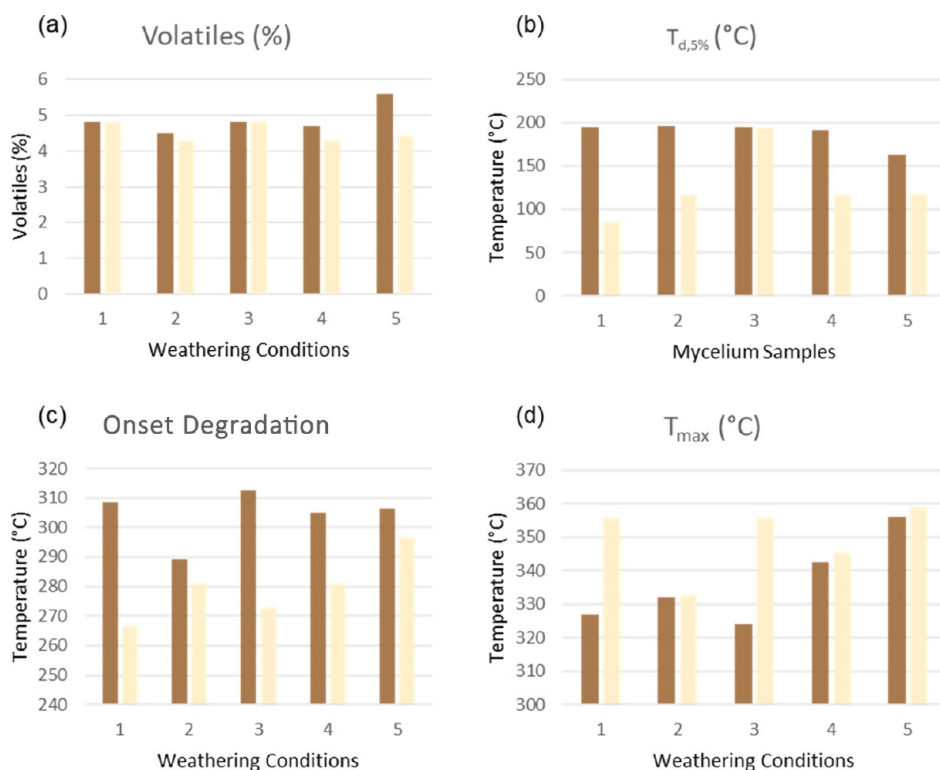


Figure 14. Comparison of TGA results of the hemp substrate (brown) and the mycelium coating (beige): control (1), hot-dry (2), hot-humid (3), cold-dry (4), and cold-humid (5). Volatile compounds up to 200 °C (a), temperature of 5% weight loss ($T_{d,5\%}$) (b), temperature of onset of degradation (T_{onset}) (c), and maximum degradation temperature (T_{max}) reveal changes in thermal stability of mycelium as a result of weathering (d).

compared to the control (B1), whereas all other conditions remained the same. These results indicate that the nature of hydration of the cellulose is affected by exposure to heat. Moreover, the amount of water absorbed (H_f) increased by 18% for condition (B5) compared to the control (B1). These results are in line with the TGA findings, which showed that sample B5 had the highest water retention of all samples. In hotter temperatures, lignin begins to soften and deteriorate;

the amount of hydroxyl groups able to be bound to water declines, causing less water absorption.⁴⁸ Unlike the brown component, the white component showed a higher temperature of water absorption under both conditions (W2) and (W5). In fact, condition W5 showed the highest temperature and H_f of all samples, suggesting that cold and humidity significantly altered the hydration behavior of the fibers. Interestingly, the amount of water absorbed under hot-humid

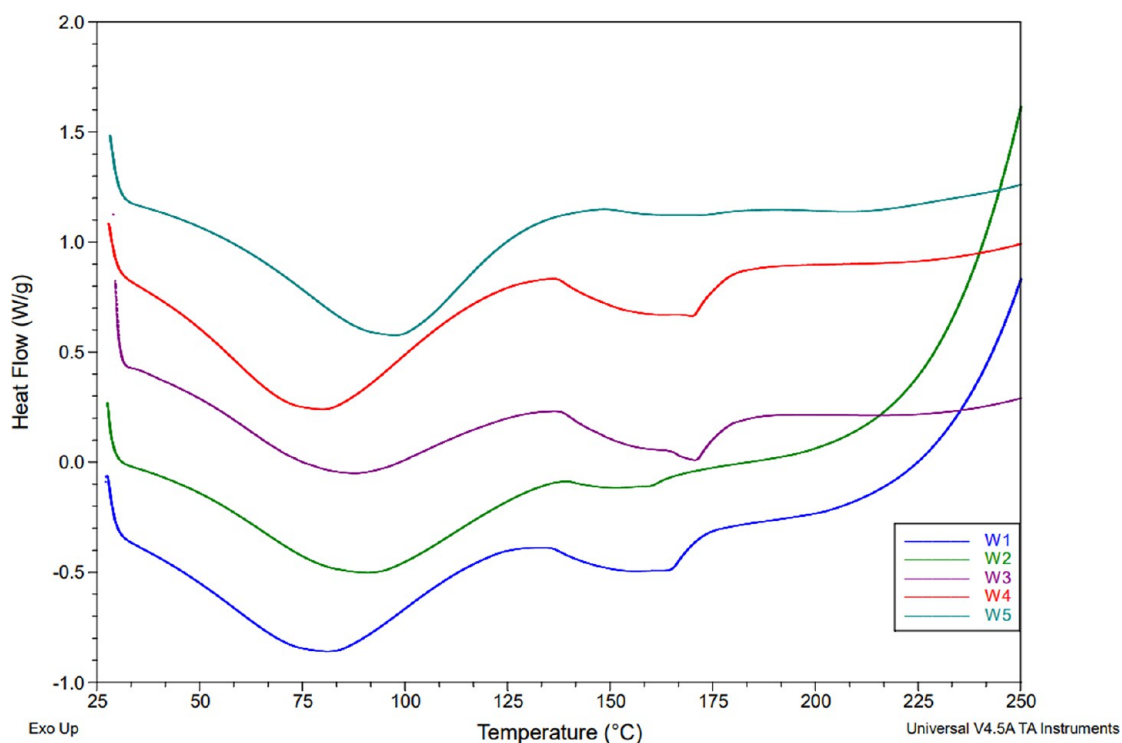


Figure 15. Comparison of DSC results of the white component: control (W1), hot-dry (W2), hot-humid (W3), cold-dry (W4), and cold-humid (W5).

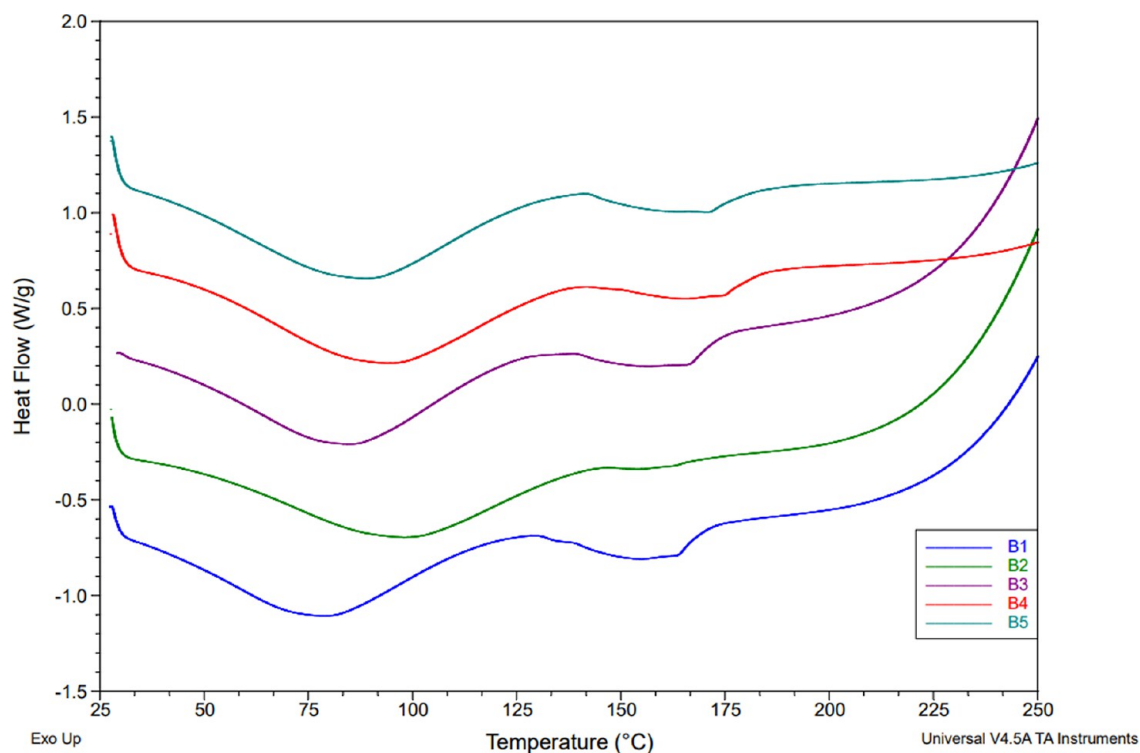


Figure 16. Comparison of DSC results of the brown component: control (B1), hot-dry (B2), hot-humid (B3), cold-dry (B4), and cold-humid (B5).

(W3) conditions decreased by one-third, revealing the combined effect of the more pronounced effect of temperature rather than humidity on the fibers.

DSC results in Figure 17c,d compare the lignin softening temperature and enthalpy. The softening temperature increases

for all samples compared to the control, with condition B5 showing the highest temperature. Moreover, the enthalpy of this transition showed a significant increase for all brown conditions except the (B2) conditions, which decreased by ~50%. Similarly, the white component also showed a 3-fold

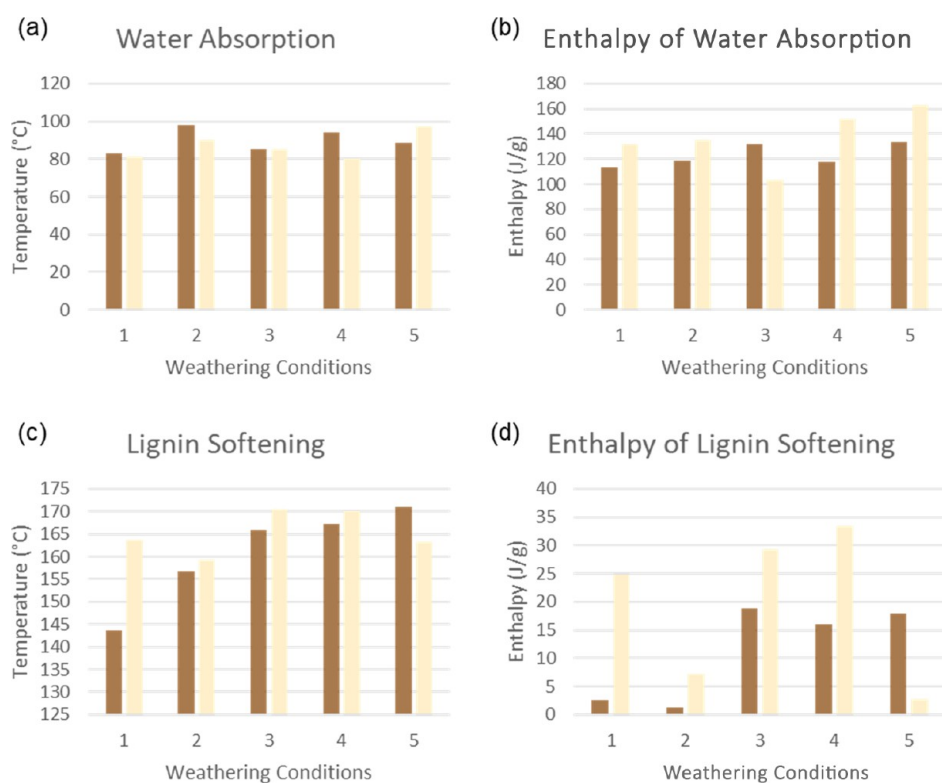


Figure 17. Comparison of DSC results of the brown substrate (dark brown) and the white mycelium coating (beige): control (1), hot-dry (2), hot-humid (3), cold-dry (4), and cold-humid (5). Water absorption (a), enthalpy associated with water absorption (b), lignin softening (c), and enthalpy associated with the lignin softening (d) reveal changes in hydration and the lignin structure of mycelium biocomposites.

Table 4. Thermal Properties of Mycelium Biocomposites

ID	condition	volatiles (%)	solids (%)	TD 5 (°C)	onset T1 (°C)	T_{\max} T1 (°C)	Wt loss T1 (%)	water desorb temp (°C)	water desorb H_f (J/g)	lignin softening temp (°C)	lignin softening H_f (J/g)
B1	control	4.8	25.5	194.7	308.4	326.8	69.3	82.9	113.1	143.6	2.6
B2	hot-dry	4.5	25.4	196.6	289.2	332.2	69.3	98.0	118.5	156.7	1.2
B3	hot-humid	4.8	17.8	195.4	312.7	324.1	71.5	85.1	132.4	165.8	18.8
B4	cold-dry	4.7	27.7	191.6	305.1	342.6	57.5	94.2	118.0	167.2	16.0
B5	cold-humid	5.6	29.1	163.4	306.4	356.2	57.2	88.7	133.8	171.0	18.0
W1	control	4.8	29.6	85.5	266.5	355.7	60.6	81.2	131.6	163.8	24.8
W2	hot-dry	4.3	30.3	117.2	281.0	332.7	79.0	90.3	135.3	159.4	7.3
W3	hot-humid	4.8	27.4	194.6	273.0	355.8	59.3	85.3	103.7	170.6	29.3
W4	cold-dry	4.3	29.2	116.6	280.8	345.2	59.5	79.9	152.0	170.0	33.5
W5	cold-humid	4.4	28.6	118.0	296.6	359.0	56.8	97.3	163.0	163.2	2.8

decrease in the enthalpy of the lignin softening under the same conditions (W2). These results suggest that high heat and humidity decrease the number of lignin interactions in the biocomposite. Under cold and humid conditions (5), the brown and white components exhibited contrasting behavior, with the fibers (W5) showing a 10-fold decrease in enthalpy, while the substrate (B5) decreased by 6-fold. These results indicate that the fibers are more sensitive to humid low temperatures, resulting in a loss of lignin softening. Conditions (W3) and (W4) exhibited an increase in the enthalpy and temperature of lignin softening compared to the control (W1).

Overall, the hot conditions decreased the amount of water absorption, whereas the humid cold conditions showed the opposite effect. Likewise, the lignin softening was found to be strongly affected by heat and humidity, which causes the lignin chain structure to enter a glassy state, where it can deform and stretch. Increased heat and the drying of the material are shown to decrease lignin softening, which was observed with

the hot-dry (2) condition.⁴⁸ Conditions (2) and (5) also appear to have the most profound negative effect on the lignin softening of both components.

MECHANICAL TESTING

Shore Hardness. Hardness testing was performed to measure the material's resistance to surface deformation. The PTC Instruments Shore D Scale Durometer was used to measure the hardness, and the results are summarized in Figure 18 and Table 5. Mechanical data in Figure 18 represent the relationship between the hardness, average energy absorbed, and density of the mycelium biocomposites.

The white mycelium layer of the control sample (W1) exhibited an average hardness of 9.7, with a reasonable standard deviation of ~18% for triplicate measurements. Dry conditions (W2) and (W4) revealed similar hardness with an increase in standard deviation. In contrast, humid conditions

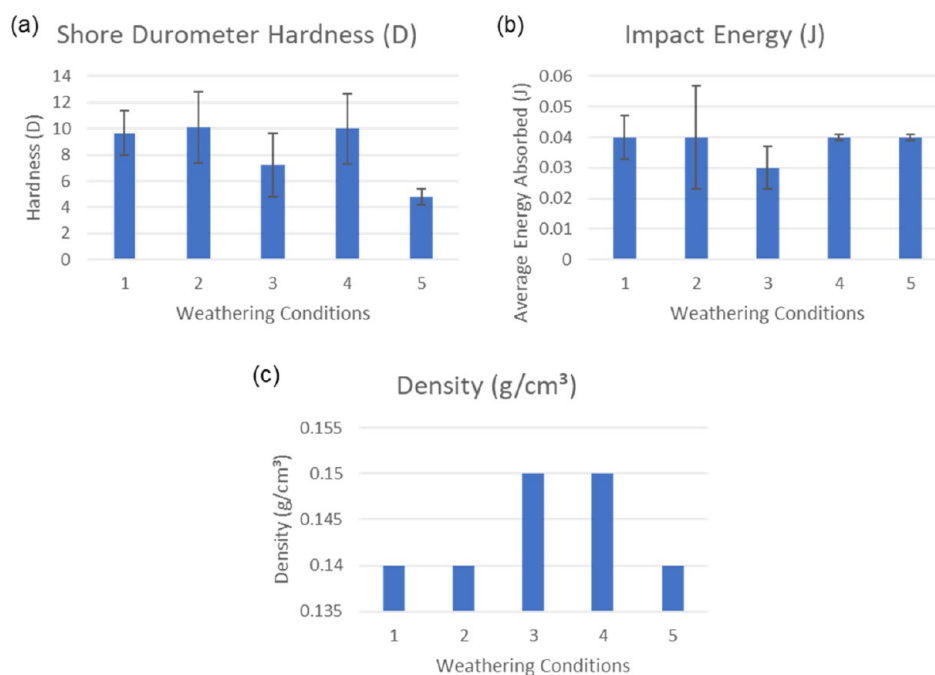


Figure 18. Comparison of mechanical results of the mycelium biocomposite: control (1), hot-dry (2), hot-humid (3), cold-dry (4), and cold-humid (5). Shore Hardness (a), impact energy (b), and density (c) reveal changes in the mechanical properties of mycelium biocomposites.

Table 5. Mechanical Properties of Mycelium Biocomposites

sample ID	condition	shore durometer hardness (<i>D</i>)	average energy absorbed (J)	density (g/cm ³)
1	control	9.7 ± 1.7	0.04 ± 0.007	0.14
2	hot-dry	10.1 ± 2.7	0.04 ± 0.017	0.14
3	hot-humid	7.2 ± 2.4	0.03 ± 0.007	0.15
4	cold-dry	10.0 ± 2.7	0.04 ± <0.001	0.15
5	cold-humid	4.8 ± 0.6	0.04 ± <0.001	0.14

(W3) and (W5) exhibited a more significant change in hardness, as shown in Figure 18, with condition (W5) decreasing by nearly 2-fold. This result is not entirely unexpected because this condition (W5) showed the highest moisture absorption in the brown component, which is expected to reduce the mechanical properties of the fibers. Consistent with the thermal results, the hot-dry (2) or cold-dry (4) conditions did not appear to affect the hardness of the mycelium fibers.

IZOD Impact Strength. An impact test was also performed on the entire composite by using an IZOD tester. Unlike changes in the mycelium fiber hardness observed due to weathering conditions, all biocomposites exhibited a similar impact strength of ~0.04 J. Only the hot-humid condition (3) showed a slight decrease in the strength to 0.03 ± 0.007 J. Figure 19 reveals that all samples broke into two pieces, as expected, revealing their brittle nature. Overall, the changes in the hardness of the mycelium fibers demonstrate that humidity exhibited a negative effect. That said, the impact strength of the entire biocomposite was not significantly affected by the loss in hardness of the fibers. These results indicate the weathering conditions did not drastically alter the mechanical properties of mycelium biocomposites.

DISCUSSION

Mycelium biocomposites were subjected to varying heat and humidity levels to evaluate the changes in their material

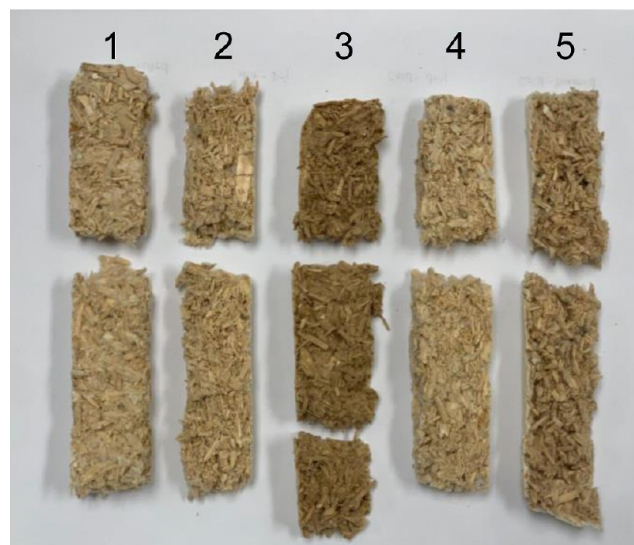


Figure 19. Trial 1 of conditions (1–5) after the Izod impact test (left to right).

properties. Morphological tests showed no significant changes in the mycelium fibers but cracking and damage of the cellulose substrate when exposed to weathering conditions. FTIR results revealed changes in the polyamide to cellulose ratios, suggesting some rearrangements in the mycelium fibers due to weathering. In addition, exposure to heat also led to protein rearrangement compared with the control sample.

The thermal properties of the biocomposite were not significantly affected by the weathering, in some cases improving. Specifically, the white component exhibited a higher thermal stability compared to the control, as indicated by increased $T_{d,5\%}$ and T_{onset} . In contrast, the brown substrate showed similar or slightly decreased thermal stability compared to the control (1). High heat conditions (2) and (3) were

found to show the strongest effect on the T_{onset} and T_{max} of the brown components. In addition, TGA demonstrated samples exposed to cold and humidity (5) exhibited the highest moisture retention. This result was confirmed with DSC analysis, which also revealed the highest water retention for both components. Interestingly, the combination of heat and humidity (3) resulted in a loss in water absorption, suggesting that temperature has a more pronounced effect than humidity. DSC analysis also revealed that conditions (2) and (5) resulted in a decrease in lignin softening of both components.

Although hardness testing of the white component demonstrated a decrease in hardness due to exposure to humidity, impact testing of the entire biocomposite did not reveal any differences. These results indicate that moisture absorption of the mycelium fibers resulted in a loss in hardness, but it did not impact the overall durability of the composite. Overall, the changes observed in our study suggest that mycelium biocomposites exhibit sufficient properties for packaging applications, even under extreme environmental conditions.

CONCLUSIONS

This study evaluated the effect of various real-world environmental conditions on the chemical, thermal, and mechanical properties of a commercially available mycelium biocomposite. We characterized the mycelium structure and detected small changes in the polymer composition and morphology, especially when exposed to high heat. Thermal properties did not show much change, except a decreased stability of the cellulosic component when exposed to high heat. Mycelium exhibited the highest moisture retention when exposed to humidity and cold, which resulted in a decrease in the mechanical properties of the fibers but did not affect the impact strength of the overall composite. Altogether, the biocomposites were robust to weathering conditions, making them appropriate for shipping applications.

ASSOCIATED CONTENT

Supporting Information

The Supporting Information is available free of charge at <https://pubs.acs.org/doi/10.1021/acsabm.4c01192>.

Data will be made available on request, additional SEM imaging at further magnification, and TGA thermograms with derivative plots (PDF)

AUTHOR INFORMATION

Corresponding Author

Dr Yanika Schneider – Department of Chemical and Materials Engineering, San José State University, San Jose, California 95192, United States; Eurofins EAG Laboratories, Sunnyvale, California 94086, United States; orcid.org/0000-0001-6806-3049; Email: yanika.schneider@sjsu.edu

Authors

Nicholas Schultz – Department of Chemical and Materials Engineering, San José State University, San Jose, California 95192, United States; orcid.org/0009-0006-6416-4364
Ajimahil Fazli – Department of Chemical and Materials Engineering, San José State University, San Jose, California 95192, United States; Eurofins EAG Laboratories, Sunnyvale, California 94086, United States

Sharmaine Piros – Department of Chemical and Materials Engineering, San José State University, San Jose, California 95192, United States

Yuritzi Barranco-Origel – Department of Chemical and Materials Engineering, San José State University, San Jose, California 95192, United States

Patricia DeLa Cruz – Department of Chemical and Materials Engineering, San José State University, San Jose, California 95192, United States; Eurofins EAG Laboratories, Sunnyvale, California 94086, United States

Complete contact information is available at: <https://pubs.acs.org/doi/10.1021/acsabm.4c01192>

Notes

The authors declare no competing financial interest.

ACKNOWLEDGMENTS

We would like to thank Dr. David Wagner and the SJSU Department of materials engineering for providing the required testing facilities to perform materials characterization. We also thank Dr. Richard Chung for supporting our project from start to finish. Finally, we thank Dr. Jennifer Hoffman and Patricia Dela Cruz of EAG Laboratories for their guidance and providing the testing facilities to perform morphological studies.

REFERENCES

- O'Shaughnessy, S. The Problem with Packaging Waste: How Zero-Waste Grocers Are Powering Solutions, Environmental and Energy Study Institute. 2020, <https://www.eesi.org/articles/view/the-problem-with-packaging-waste-how-zero-waste-grocers-are-powering-solutions>.
- Gibb, B. C. Plastics are forever. *Nat. Chem.* **2019**, *11* (5), 394–395.
- Hidalgo-Crespo, J.; Soto, M.; Amaya-Rivas, J.; Santos-Méndez, M. Carbon and water footprint for the recycling process of expanded polystyrene (EPS) post-consumer waste. *Procedia CIRP* **2022**, *105*, 452–457.
- Enarevba, D. R.; Haapala, K. R. A comparative life cycle assessment of expanded polystyrene and mycelium packaging box inserts. *Procedia CIRP* **2023**, *116*, 654–659.
- Chan, H. H. S.; Not, C. Variations in the spatial distribution of expanded polystyrene marine debris: Are Asian's coastlines more affected? *Environ. Adv.* **2023**, *11*, 100342.
- Jang, M.; Shim, W. J.; Han, G. M.; Rani, M.; Song, Y. K.; Hong, S. H. Styrofoam debris as a source of hazardous additives for marine organisms. *Environ. Sci. Technol.* **2016**, *50* (10), 4951–4960.
- Geyer, R.; Jambeck, J. R.; Law, K. L. Production, use, and fate of all plastics ever made. *Sci. Adv.* **2017**, *3* (7), No. e1700782.
- Alimi, O. S.; Budarz, J. F.; Hernandez, L. M.; Tufenkji, N. Microplastics and Nanoplastics in Aquatic Environments: Aggregation, Deposition, and Enhanced Contaminant Transport. *Environ. Sci. Technol.* **2018**, *52* (4), 1704–1724.
- Bharath, K. M.; Muthulakshmi, A.; Natesan, U. Microplastic contamination around the landfills: Distribution, characterization and threats: A review. *Curr. Opin. Environ. Sci. Health* **2023**, *31*, 100422.
- da Silva, E. F.; do Carmo, D. d. F.; Muniz, M. C.; dos Santos, C. A.; Cardozo, B. B. I.; Costa, D. M. d. O.; dos Anjos, R. M.; Vezzone, M. Evaluation of microplastic and marine debris on the beaches of Niterói Oceanic Region, Rio De Janeiro, Brazil. *Mar. Pollut. Bull.* **2022**, *175*, 113161.
- Peng, L.; Yi, J.; Yang, X.; Xie, J.; Chen, C. Development and characterization of mycelium bio-composites by utilization of different agricultural residual byproducts. *J. Bioresour. Bioprod.* **2023**, *8* (1), 78–89.

- (12) Kandel, B. Mycelium: Using Mushrooms for the Future Packaging Materials in Europe; Tampere University of Applied Sciences, Bachelor's dissertation, Theseus, 2021. <https://www.theseus.fi/handle/10024/748056>.
- (13) Birn, A. Specialty mushroom cultivation—Cornell Small Farms; Cornell Small Farms Program, 2020. <https://smallfarms.cornell.edu/projects/mushrooms/specialty-mushroom-cultivation/>.
- (14) The Life Cycle Of A Mushroom Explained. Natura Mushrooms. 2021, <https://naturamushrooms.com/blogs/news/the-life-cycle-of-a-mushroom>.
- (15) Mushroom Research Center Austria. Pleurotus ostreatus; Mushroom Research Center Austria. <http://mrca-science.org/index.php/en/mushroom-cultivation/43-zuchtanl>.
- (16) MycoHaus. Fruiting your Substrate; MycoHaus. <https://www.mycnhaus.com/pages/fruited-your-substrate>.
- (17) Sivaprasad, S.; Byju, S. K.; Prajith, C.; Shaju, J.; Rejeesh, C. Development of a novel mycelium bio-composite material to substitute for polystyrene in packaging applications. *Mater. Today: Proc.* **2021**, *47* (15), 5038–5044.
- (18) Manan, S.; Ullah, M. W.; Ul-Islam, M.; Atta, O. M.; Yang, G. Synthesis and applications of fungal mycelium-based advanced functional materials. *J. Bioresour. Bioprod.* **2021**, *6* (1), 1–10.
- (19) Geyman, M. How Mushrooms Could Help Solve the Beauty Industry's Waste Problem; Vogue, 2020. <https://www.vogue.com/article/mycelium-packaging-could-help-solve-beauty-industry-waste-problem>.
- (20) Grown bio. About. Grown bio, 2022. <https://www.grown.bio/about/>.
- (21) Attias, N.; Danai, O.; Abitbol, T.; Tarazi, E.; Ezov, N.; Pereman, I.; Grobman, Y. J. Mycelium bio-composites in industrial design and architecture: Comparative review and experimental analysis. *J. Clean. Prod.* **2020**, *246*, 119037.
- (22) Haneef, M.; Ceseracciu, L.; Canale, C.; Bayer, I. S.; Heredia-Guerrero, J. A.; Athanassiou, A. Advanced Materials From Fungal Mycelium: Fabrication and Tuning of Physical Properties. *Sci. Rep.* **2017**, *7*, 41292.
- (23) Antinori, M.; Ceseracciu, L.; Mancini, G.; Heredia-Guerrero, J. A.; Athanassiou, A. Fine-Tuning of Physicochemical Properties and Growth Dynamics of Mycelium-Based Materials. *ACS Appl. Biomater.* **2020**, *3* (2), 1044–1051.
- (24) Abhijith, R.; Ashok, A.; Rejeesh, C. Sustainable packaging applications from mycelium to substitute polystyrene: a review. *Mater. Today: Proc.* **2018**, *5* (1), 2139–2145.
- (25) McKenzie, J. Unpacking the packaging potential of mycelium, the mushroom “roots” of many uses. *Bull. At. Sci.* 2023. <https://thebulletin.org/2023/01/unpacking-the-packaging-potential-of-mycelium-the-mushroom-roots-of-many-uses/>.
- (26) Yang, L.; Park, D.; Qin, Z. Material function of mycelium-based bio-composite: A review. *Front. Mater.* **2021**, *8*, 737377.
- (27) Muiruri, J.; Yeo, J. C. C.; Zhu, Q.; Ye, E.; Loh, X. J.; Li, Z. Sustainable Mycelium-Bound Biocomposites: Design Strategies, Materials Properties, and Emerging Applications. *ACS Sustain. Chem. Eng.* **2023**, *11* (18), 6801–6821.
- (28) Jose, J.; Uvais, K. N.; Sreenadh, T. S.; Deepak, A. V.; Rejeesh, C. R. Investigations into the Development of a Mycelium Biocomposite to Substitute Polystyrene in Packaging Applications. *Arab J. Sci. Eng.* **2021**, *46*, 2975–2984.
- (29) Chan, X. Y.; Saeidi, N.; Javadian, A.; Hebel, D. E.; Gupta, M. Mechanical properties of dense mycelium-bound composites under accelerated tropical weathering conditions. *Sci. Rep.* **2021**, *11*, 22112.
- (30) Gao, Y.; Huang, C.; Chen, Y.; Chen, X.; Shen, Y.; Yu, H. Y. Sustainable production of in-situ CO₂ capture and mineralization of multifunctional nanowood with excellent anisotropic, flame retardant, and durability for building construction. *Ind. Crops Prod.* **2024**, *221*, 119353.
- (31) Ji, H.; Abdalkarim, S. Y. H.; Shen, Y.; Chen, X.; Zhang, Y.; Shen, J.; Yu, H. Y. Facile synthesis, release mechanism, and life cycle assessment of amine-modified lignin for bifunctional slow-release fertilizer. *Int. J. Biol. Macromol.* **2024**, *278* (Part 2), 134618.
- (32) Packaging Ecovative, <https://www.ecovative.com/pages/packaging>.
- (33) Engineering. ToolBox. Saturated Salt Solutions and control of Air Humidity, 2014. [online] Available at: https://www.engineeringtoolbox.com/salt-humidity-d_1887.html.
- (34) Kurara, H. *An Introduction of Below-Freezing and Humidity Environment Controlling Technology Equipped on Brake Test Equipment*. Report No. 25; ESPEC Technical Information, ESPEC Corp, 2017.
- (35) Callister, W. D. *Materials Science and Engineering: An Introduction*; John Wiley & Sons: Hoboken, NJ, 2007.
- (36) Intertek. Shore Hardness ASTM D2240, <https://www.intertek.com/polymers/testlopedia/shore-hardness-astm-d2240/>.
- (37) Intertek. Izod Impact (Unnotched) ASTM D4812, ISO 180, <https://www.intertek.com/polymers/testlopedia/unnotched-izod-impact-astm-d4812/>.
- (38) Elsacker, E.; Vandeloock, S.; Brancart, J.; Peeters, E.; De Laet, L. Mechanical, physical and chemical characterisation of mycelium-based composites with different types of lignocellulosic substrates. *PLoS One* **2019**, *14* (7), No. e0213954.
- (39) Joshi, K.; Meher, M. K.; Poluri, K. M. Fabrication and Characterization of Bioblocks from Agricultural Waste Using Fungal Mycelium for Renewable and Sustainable Applications. *ACS Appl. Biomater.* **2020**, *3* (4), 1884–1892.
- (40) Bustillos, J.; Loganathan, A.; Agrawal, R.; Gonzalez, B. A.; Perez, M. G.; Ramaswamy, S.; Boesl, B.; Agarwal, A. Uncovering the Mechanical, Thermal, and Chemical Characteristics of Biodegradable Mushroom Leather with Intrinsic Antifungal and Antibacterial Properties. *ACS Appl. Biomater.* **2020**, *3* (5), 3145–3156.
- (41) Appels, F. V.; Camere, S.; Montalti, M.; Karana, E.; Jansen, K. M.; Dijksterhuis, J.; Krijgsheld, P.; Wösten, H. A. Fabrication factors influencing mechanical, moisture- and water-related properties of mycelium-based composites. *Mater. Des.* **2019**, *161*, 64–71.
- (42) Sun, W.; Tajvidi, M.; Hunt, C. G.; Howell, C. All-Natural Smart Mycelium Surface with Tunable Wettability. *ACS Appl. Bio Mater.* **2021**, *4* (1), 1015–1022.
- (43) Girometta, C.; Picco, A. M.; Baiguera, R. M.; Dondi, D.; Babbini, S.; Cartabia, M.; Pellegrini, M.; Savino, E. Physico-mechanical and thermodynamic properties of mycelium-based biocomposites: a review. *Sustainability* **2019**, *11* (1), 281.
- (44) Alves, R.; Alves, M. L.; Campos, M. J. Morphology and Thermal Behaviour of New Mycelium-Based Composites with Different Types of Substrates. *Prog. Digit. Phys. Manuf.* **2020**, 189–197.
- (45) Stevulova, N.; Estokova, A.; Cigasova, J.; Schwarzova, I.; Kacik, F.; Geffert, A. Thermal degradation of natural and treated hemp hurds under air and nitrogen atmosphere. *J. Therm. Anal. Calorim.* **2017**, *128*, 1649–1660.
- (46) Gou, L.; Li, S.; Yin, J.; Li, T.; Liu, X. Morphological and physico-mechanical properties of mycelium biocomposites with natural reinforcement particles. *Constr. Build. Mater.* **2021**, *304*, 124656.
- (47) Yang, H.; Yan, R.; Chen, H.; Lee, D. H.; Zheng, C. Characteristics of Hemicellulose, Cellulose and Lignin Pyrolysis. *Fuel* **2007**, *86*, 1781–1788.
- (48) Böröcsök, Z.; Pásztor, Z. The role of lignin in wood working processes using elevated temperatures: an abbreviated literature survey. *Eur. J. Wood Prod.* **2021**, *79*, 511–526.